

See discussions, stats, and author profiles for this publication at: <https://www.researchgate.net/publication/288212459>

Influence of connection detailing on strength of concrete-filled FRP tubes under bending and shear

Article · January 2011

CITATIONS

0

READS

19

3 authors, including:



Pedram Sadeghian

Dalhousie University

28 PUBLICATIONS 78 CITATIONS

[SEE PROFILE](#)



Amir Fam

Queen's University

189 PUBLICATIONS 2,037 CITATIONS

[SEE PROFILE](#)

Some of the authors of this publication are also working on these related projects:



Experimental and numerical assessment of the behavior of slender concrete columns reinforced with GFRP, and steel RC columns strengthened with longitudinal CFRP strips using bonded or near surface mounted (NSM) technique [View project](#)



Connections of Concrete-Filled FRP Tubes to Concrete Members [View project](#)

All content following this page was uploaded by [Pedram Sadeghian](#) on 03 April 2017.

The user has requested enhancement of the downloaded file.

Influence of connection detailing on strength of concrete-filled FRP tubes under bending and shear

Sarah Zakaib, Pedram Sadeghian, and Amir Fam

Synopsis: In this study, five specimens comprising concrete-filled glass fibre-reinforced polymer (GFRP) tubes (CFFTs) with and without moment connections to concrete footings were tested. The study aims at exploring the effect of combined maximum shear and moment, both occurring at the same location, on the ultimate moment capacity of the CFFT system, as well as the behaviour of the moment connection in general. Testing involved three-point and four-point bending of simply supported specimens as well as cantilever bending tests with varying shear spans and fixed end arrangements. The end conditions of the CFFTs consisted of either direct embedment into concrete blocks with steel dowels or mechanical clamping of the fixed end. For the GFRP tubes used, the study concluded that the presence of shear at the location of maximum moment near the connection in a cantilever setup does not cause reduction in flexural capacity, relative to the pure bending strength of the CFFT. This confirms a similar conclusion reported in literature for simply supported CFFT beams without end constraints. The study also revealed that achieving tensile rupture of the tube does not guarantee that the full potential moment capacity of the CFFT member is reached, as slip plays a key role at the moment connection.

Keywords: CFFT, footing, combined loading, connection, flexure, FRP, shear, tubes

Sarah Zakaib is a Master's Candidate in the Department of Civil Engineering at Queen's University, Kingston, Canada.

Pedram Sadeghian is a Postdoctoral Fellow in the Department of Civil Engineering at Queen's University, Kingston, Canada. His research interests include the use of innovative materials and systems such as fibre reinforced polymers for existing and new concrete structures.

ACI Member **Amir Fam** is a Professor and Canada Research Chair in Innovative and Retrofitted Structures at Queen's University, Canada. He is a voting member of ACI Committee 440, Fiber Reinforced Polymer (FRP) Reinforcement, and chair of Sub-Committee 440-J, FRP Stay-in-Place Formwork. His research interests include applications of FRPs in new concrete construction and rehabilitation of existing structures.

INTRODUCTION

The deterioration of infrastructure has led to new methods and materials for construction that are more durable. Early on, it was demonstrated that rehabilitation of aging infrastructure by wrapping concrete members with fibre reinforced polymers (FRPs) is an accepted method of increasing their strength (Fardis and Khalili 1981). FRP tubes, which are commercially available for the pipeline industry, have a great potential as a stay-in-place forms that can be filled with concrete and used in a variety of structural applications. This includes bridge piers, piles and utility poles. Early research by Mirmiran and Shahawy (1997) demonstrated that the concrete-filled FRP tube (CFFT) system can significantly enhance strength and ductility of columns through confinement and control of the dilation of concrete. Additionally, the FRP tube protects the concrete core from external aggressive environments. The CFFT system has also been studied in flexure and under combined flexural and axial loading (Fam et al. 2003(a)) and field installation of CFFTs as bridge piers occurred in the Route 40 Bridge in Virginia (Fam et al. 2003(b)). A study on CFFT pile driving has shown the feasibility and success of driving CFFT piles using conventional equipment in the field (Helmi et al. 2005).

Several studies have been carried out on CFFT connections to concrete footings. Zhu et al. (2004 and 2006) studied various connections of CFFT columns to concrete footings. In these studies, internal steel reinforcement was continuous through the full height of the CFFT members and embedded through the footing. Nelson et al. (2008) studied a moment connection by direct embedment of the CFFT into the footing without any steel reinforcement. This paper examines the behaviour of CFFTs connected to concrete footings through a combination of direct embedment of the CFFT into the footing and steel dowels connecting the footing to the CFFT. The steel dowels only extend into the CFFT within the portion embedded into the footing. Earlier research by Ahmad et al. (2008) on the shear strength of CFFT members without internal longitudinal steel reinforcement in a simple beam setup revealed that shear failure did not occur in

short CFFT beams and that flexural strength was not compromised. This study addresses the effect of combined flexure and shear on the strength of the CFFT member in a cantilever setup, including the influence of the connection arrangement.

EXPERIMENTAL PROGRAM

Specimen Layout

Five CFFT specimens were fabricated and tested to determine the influence of combined flexural and shear loading on their strength as well as the capacity of the moment connection. Two of the CFFT specimens were tested as simply supported beams in bending (Specimens B1 and B2), whereas the other three specimens were tested as cantilevers (Specimens C1, C2, and C3). Details of the specimens are given in Table 1. All specimens were created using tubes that had an outer diameter of 219 mm.

Table 1 – Test matrix.

Spec. ID	Loading Type	Span (mm)	Shear Span * D	Embedment (mm)	f'_c (MPa)
B1	4-point bending	1900	N/A	300	41
B2	3-point bending	1000	2.25D	N/A	30
C1	Cantilever	1040	4.75D	260	36
C2	Cantilever	1600	7.25D	260	34
C3	Cantilever	1040	4.75D	(clamped) 610	30

B1 – In all previous research on CFFT members tested in flexure, three- or four-point bending tests were carried out where the CFFT member extends from the constant moment region into the shear span. Often, failure occurred just under one of the loading points and hence it is difficult to isolate the effects of flexure and shear. In this study, Specimen B1 was designed such that a CFFT segment is subjected to pure bending within a constant moment region, without the influence of shear, and is shown in Figure 1. The specimen was a simple beam loaded in four-point bending. The shear spans extending over the end supports consisted of heavily reinforced concrete blocks, 800 mm (31-1/2 in) long, with a square cross-section of 400x400 mm (15-3/4 x 15-3/4 in). The CFFT tube was located within the constant moment region and embedded 300 mm (11-13/16 in) on each side into the concrete blocks. The clear length of the CFFT member within the constant moment region was 660 mm (26 in) or 3D, where D is the outer tube diameter. The span between supports was 1900 mm (74-3/16 in), with a shear span of 500 mm (19-5/8 in) long on each side and a constant moment zone of 900 mm (35-7/16 in) between the loading points, which ensures that the entire CFFT clear length is subject to pure bending.

B2 – Specimen B2 was loaded in three-point bending with unrestrained ends (i.e. no concrete blocks and slip between the tube and concrete core is unrestrained), as shown in Figure 2. The span length was 1000 mm (39-3/8 in), giving a shear span of 500

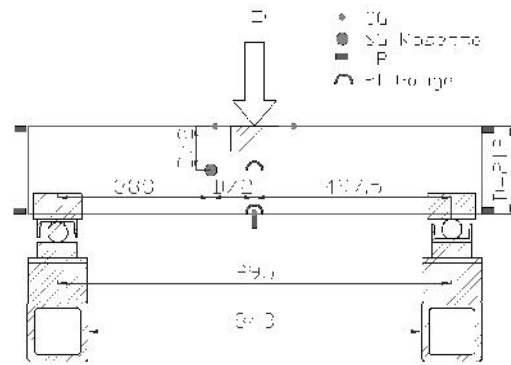


Figure 2 - Test setup of specimen B2 (all dimensions in mm).

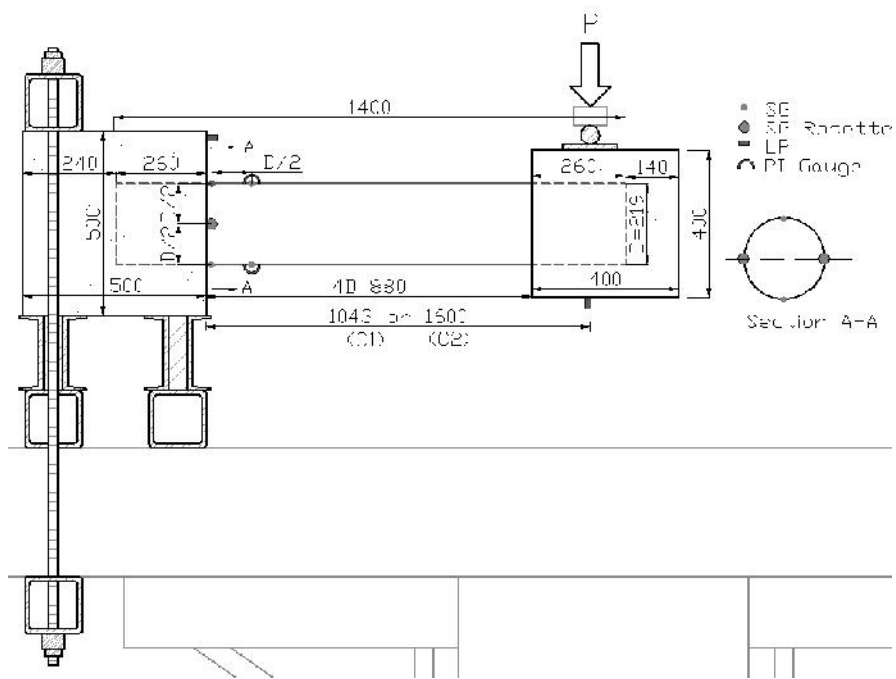


Figure 3 - Test setup of specimens C1 and C2 (all dimensions in mm).

C3 – Specimen C3 had the same span as specimen C1, 1040 mm (41 in) or 4.75D, and was also a cantilever specimen. The difference is that fixed end for this specimen is the result of mechanical clamping of the tube between two plaster-filled steel channel sections. The tube was clamped over a length of 610 mm (24 in) and loaded directly at the other end where a short overhang of 482 mm (19 in) was provided to allow for rotation of the beam. Figure 4 shows a schematic of the test setup. The objective of testing specimen C3 was to see the effect on the moment capacity of a close-to-perfect fixed end where no slip would occur, and compare this behaviour to an equal span specimen C1 that has a practical moment connection to a concrete footing. Also, specimen C3 is compared to a specimen that was tested by Mitchell and Fam (2010), with the same tube and fixed end arrangement, but with a 2665 mm (105 in) or 12.2D span, to examine the effect of shear span-to-diameter ratio.

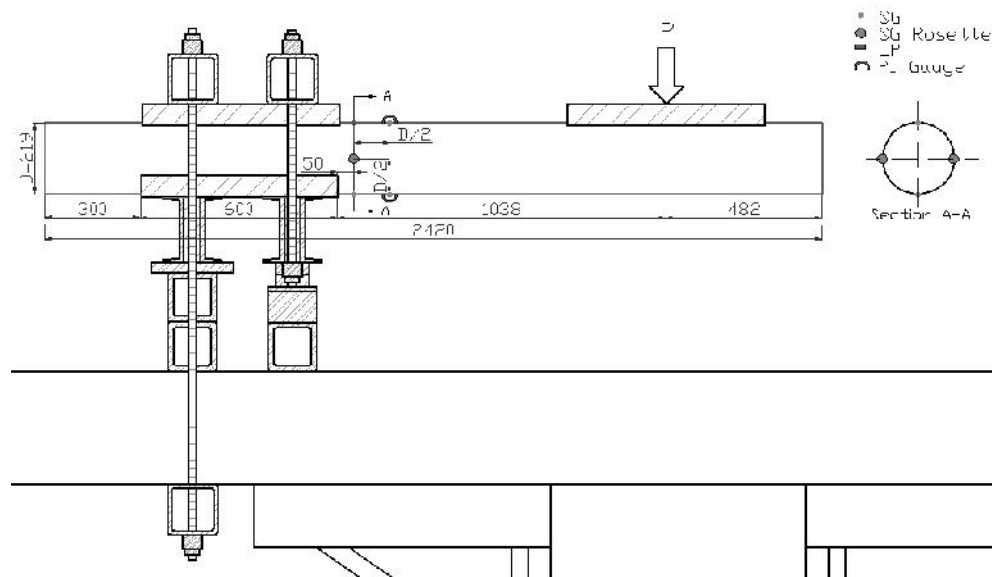


Figure 4 - Test setups of specimen C3 and specimen tested by Mitchell and Fam (2010). All dimensions in mm.

Material Properties

Tubes – The tubes used for all tests were identical. The E-glass and epoxy tubes were fabricated by Ameron International, in the Bondstrand 3200 pipes series for transmission of fluids. They have an outer diameter of 219 mm (8-5/8 in) and wall thickness of 4.3 mm (slightly more than 1/8 in), in a 7-ply [-86/+6/-86/+6/-86/+6/-86] lay-up alternating layers of hoop and longitudinal fibres. The angles of each layer (in degrees) are described with respect to the longitudinal axis of the tube. Tensile tests were performed on coupons cut from the tube in the longitudinal direction. The coupons had a width of 25 mm (1 in), tabs that are 115 mm (4-1/2 in) long at both ends, and 37 mm (1-

1/2 in) gauge length between grips. The small gauge length was chosen to decrease the effect of the discontinuous fibres wound at 6° from the longitudinal axis of the tube, following the recommendations by Mandal (2004) that a shorter coupon will result in closer behaviour and failure strain to that of the full tube. Electric resistance strain gauges were placed on either side of the coupon at the centre of the gauge length. Figure 5 shows the stress-strain curve of the GFRP tube in tension, which is somewhat bilinear, with an initial modulus of 19.5 GPa (2828 ksi). The ultimate strength and strain were 250 MPa (36.3 ksi) and 0.0205, respectively. The modulus changed to 10.7 GPa (1552 ksi) at a stress of 43 MPa (6.2 ksi) and a strain of 0.0045.

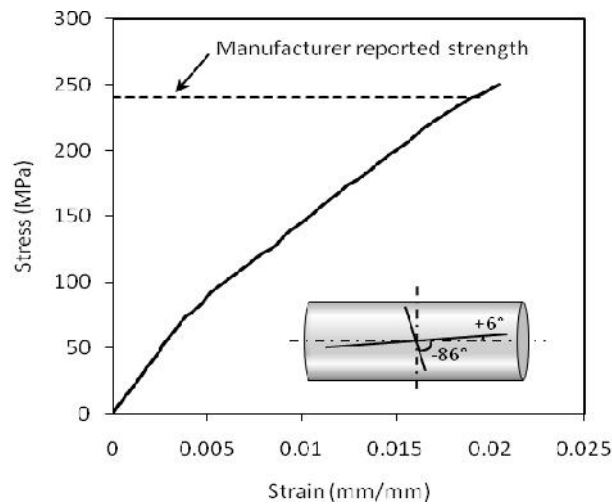


Figure 5 – Stress-strain curve of tubes from coupon testing.

Concrete – Table 1 shows the concrete compressive strength based on standard concrete cylinder tests at the time of the test. The concrete strength varied from 30 to 41 MPa (4.35 to 5.9 ksi). A previous study by Fam and Rizkalla (2003) showed that the influence of concrete strength on flexural strength of CFFT members is insignificant, which is quite different from the case of axially loaded CFFT members in compression, due to the confinement effect. For the concrete blocks, the compressive strength at the time of testing ranged from 29 to 31 MPa (4.4 ksi on average).

Steel – Grade 400W steel reinforcing bars were used in specimens B1, C1, and C2. A combination of 10M and 15M bars were used for longitudinal and transverse reinforcement in the concrete blocks. Four 20M dowels, bent at 90° , were used to connect each tube to the concrete blocks. The dowels were extended into the tube a distance equal to the embedment length of the tubes in the concrete blocks.

Fabrication

Specimens B1, C1, and C2 were all fabricated at the same time, in two separate stages. The first stage involved filling the tubes whilst in an upright position and inserting

the dowels into each end. The tubes were then laid horizontally into the formwork of the end blocks and the concrete was poured at a later stage. This practice was carried out for convenience in the lab, but for practical applications, the footing will be cast before filling the tube. Figure 6 shows the typical fabrication process for specimen B1. Specimens B2 and C3 were simply filled with concrete in an upright position.

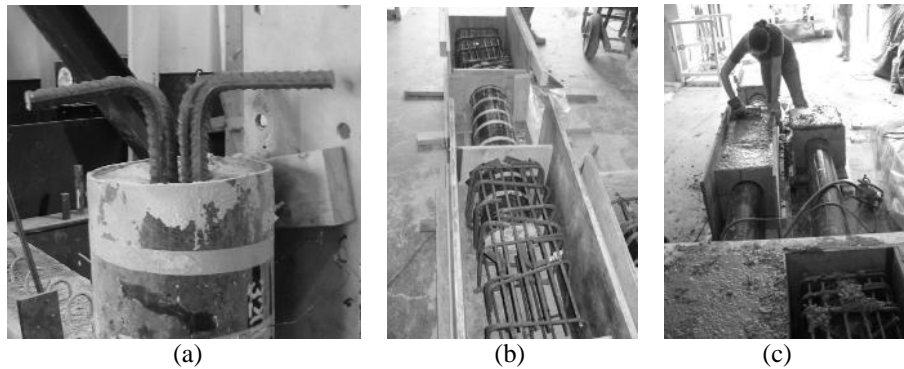


Figure 6 - Fabrication of specimen B1: a) CFPT with end dowels, b) reinforcement of end blocks, and c) casting the end block.

Test Set-up

Figures 1 to 4 show the test setups of all specimens. In testing specimen B1 as a simple beam, the loading and supporting points were all relative to the two rigid concrete prisms, ensuring pure bending over the CFPT segment. A hinged support was provided at one end while a roller support was provided at the other end. Specimen B2 was also simply supported, using a hinge and roller at either end. A plaster-filled short steel channel section was used at each support and at the loading point to conform to the round surface of the CFPT of specimen B2. For cantilever specimens C1 and C2, the concrete blocks at the fixed ends were clamped using a heavy HSS steel section, anchored to the machine using 25 mm (1 in) diameter high-strength threaded rods. Specimen C3 was also clamped using HSS sections anchoring the steel channel sections to the machine. Figure 7 shows pictures of the test setups of all specimens. A 900 kN (202 kips) capacity mechanical testing machine was used to test all specimens under stroke control.

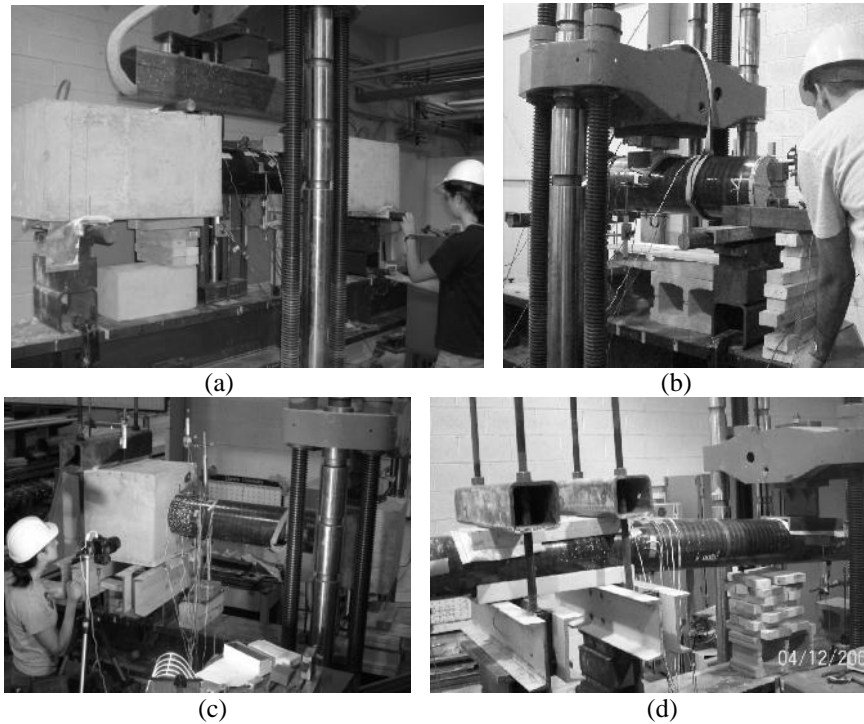


Figure 7 – Test setups for specimens: (a) B1, (b) B2, (c) C1 and C2 and (d) C3.

Instrumentation

Strain measurements were taken using electrical resistance strain gauges and position indicator (PI) gauges. Deflection and slip measurements were taken using linear potentiometers (LPs). The locations of all instrumentation can be seen for each test in Figures 1 to 4. Load was measured through a load cell built in to the machine.

TEST RESULTS

Figure 8 shows the load-deflection responses of all test specimens, while Figure 9 shows the load-longitudinal strain responses at the maximum moment regions. In the following sections, failure modes and the behaviour are discussed in detail.

Failure Modes

Specimen B1 reached a load level very close to that corresponding to flexural failure of the CFFT member, as evident by the tensile strains in Figure 9; however, slip occurred between the CFFT member and the concrete block portion, leading to significant load drop. Slip was associated with radial cracking of the concrete block as

shown in Figure 10(a). However, as indicated from the tensile strains, flexural tension failure was quite imminent. The tensile strain in the tube at failure was 0.0199, while the average tensile failure strain of the tube from the coupon tests is 0.0205. Specimen B2 failed in tension at mid-span by rupture of the GFRP tube, as shown in Figure 10(b). The strain at failure was 0.0243. Some slip occurred between the concrete core and the tube, as shown in Figure 11(a).

All three cantilever specimens (C1, C2, and C3) failed through tensile rupture of the tube, as shown in Figure 10(b). Figure 12 shows the load-slip responses of cantilever specimens C1 and C2. The slip is measured between the GFRP tube and the concrete footing; essentially the tube is pulled out of the concrete block. It is clear that slip in specimen C2 was significantly larger than that of C1. Clearly, there appears to be a correlation between the span length and the amount of slip, as the fixed end arrangements were identical in both specimens. Specimen C2 slipped significantly more than specimen C1, as shown in Figure 11(b), and both footings had some radial cracks.

Specimen C3, which was not embedded in a concrete footing but rather clamped mechanically, failed also by rupture in tension at the highest moment capacity of all three cantilever specimens, though very close to that of C1 and B1. No slip was observed in specimen C3, and it failed at a tensile strain of 0.0240.

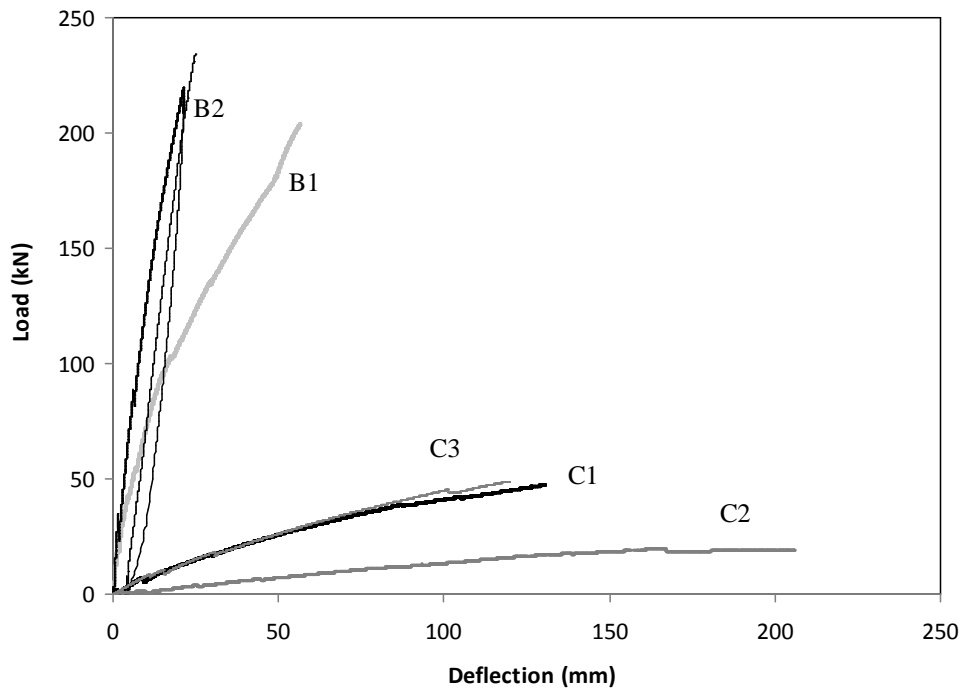


Figure 8 – Load-deflection behaviour of test specimens.

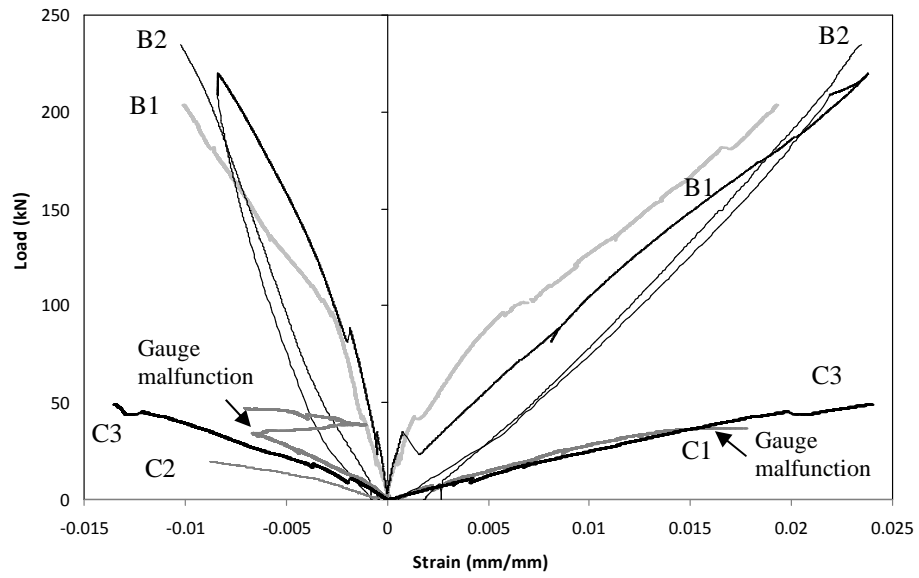


Figure 9 – Load-strain behaviour of test specimens.

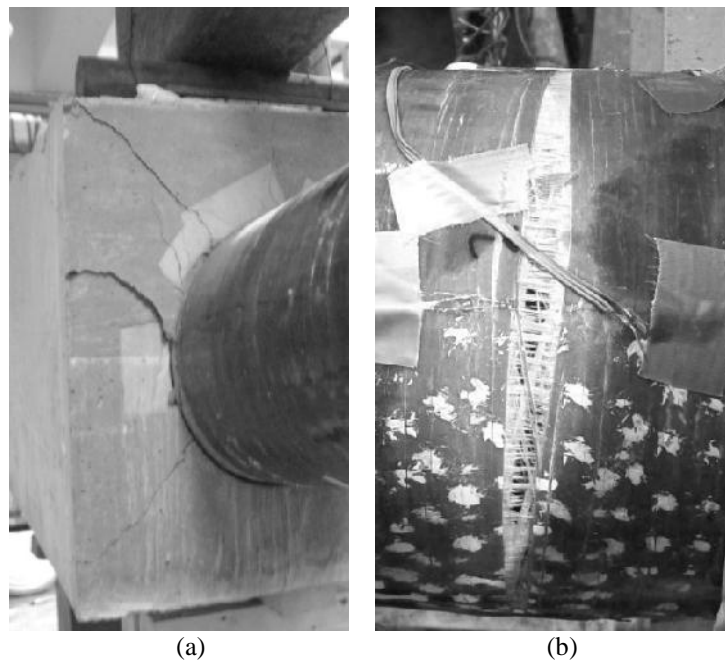


Figure 10 - Failure modes of (a) Specimen B1 and (b) Specimens B2 and C1 to C3.

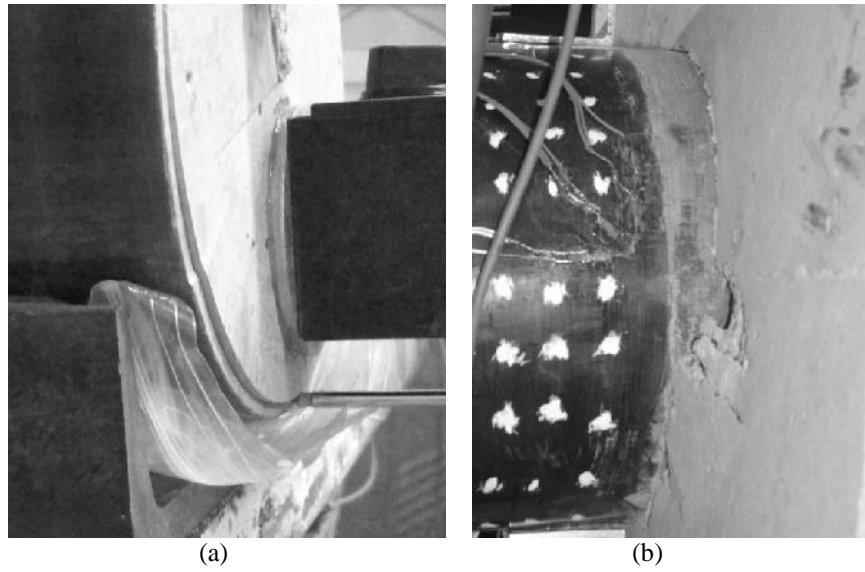


Figure 11 – (a) Internal CFFT concrete slip, and (b) External CFFT concrete slip.

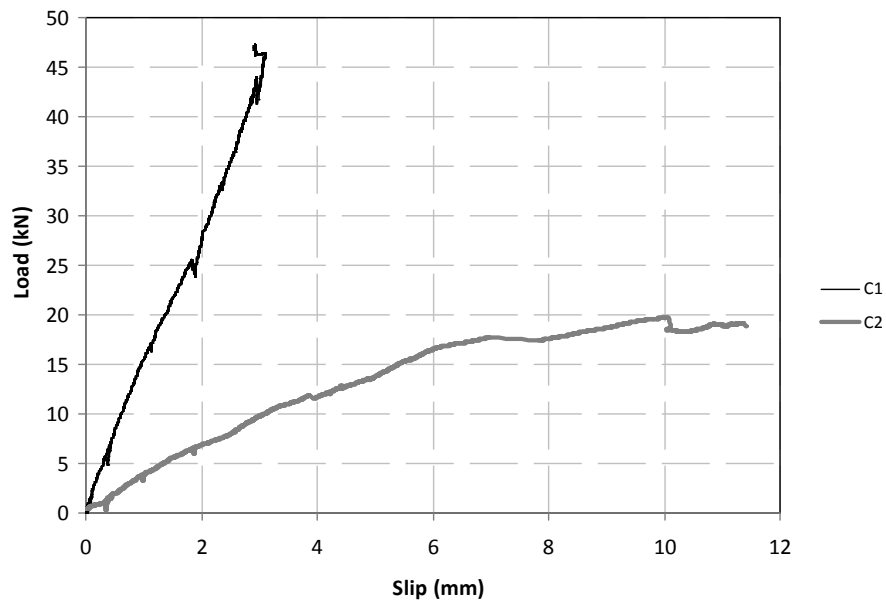


Figure 12 – Load-slip behaviour of specimens C1 and C2.

Moment-Curvature Responses

Since the boundary conditions and spans varied among the test specimens, the behaviour of the different specimens is compared based on the moment-curvature responses. The moment-curvature behaviour of the five specimens is shown in Figure 13. The curvature was determined as the slope of the strain profile at the maximum moment locations. Generally, all specimens showed similar behaviour, with the first cracking occurring around a moment of 10 kN.m (88.5 kip-in). This is followed by a reduction in stiffness and slightly nonlinear behaviour. The nonlinear behaviour results from the combined effects of concrete nonlinearity, increased cracking and the tube bi-linear stress-strain behaviour associated with splitting of the hoop fibres. Over the entire set of tests, the maximum moment achieved was 59.4 kN.m (525.7 kip-in) for Specimen B2 and the average moment was 53.4 kN.m (472.6 kip-in), not including specimen C2. Specimen C2 failed at a significantly lower moment of 31.5 kN.m (278.8 kip-in), showing a 40% reduction in capacity relative to the other specimens.

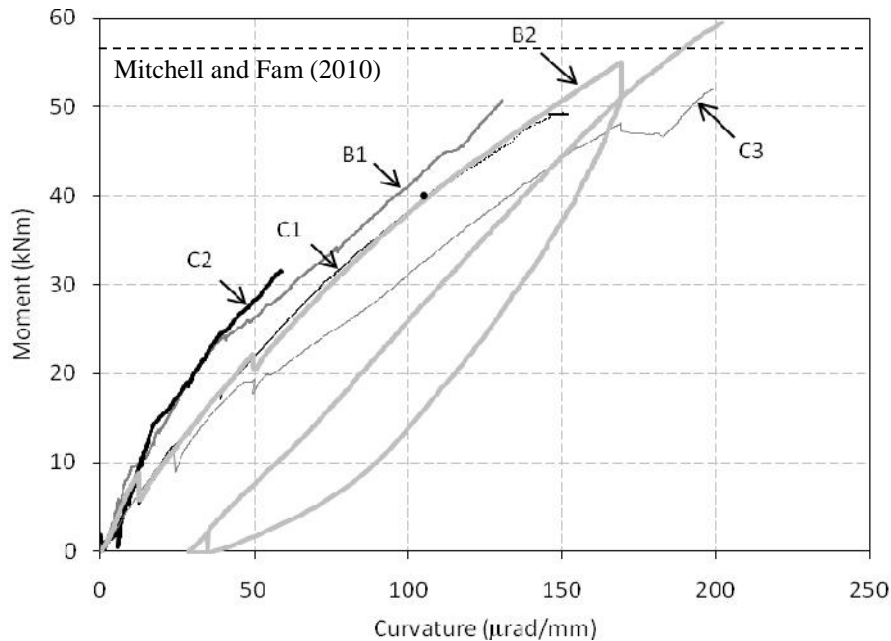


Figure 13 – Moment-curvature behaviour of test specimens.

It is worth noting that identical CFFT of the same tube used in this study and a concrete fill of 44 MPa (6.4 ksi) compressive strength was tested by Fam and Mitchell (2010), using a setup similar to that of specimen C3 of this study but with a span of 2.665 m (8.8 ft), which is equivalent to 12.2D. That specimen had flexural tension failure by rupture of the tube at a moment of 56.9 kN.m (504 kip.in). The shear span of this specimen is long enough to assure that shear did not affect the flexural strength of the

specimen. Also, the moment capacity of this specimen is quite consistent with the value obtained in this study for specimen B1, based on a slight extrapolation of the load-strain response to hypothetically reach the rupture strain of the tube, which although was imminent, was not reached because of the slip failure. In the same study by Fam and Mitchell (2010), a hollow tube was also tested under the same conditions and achieved 29.63 kN.m (262 kip.in), giving the lower bound strength of the system. This information will shed light on the behaviour of the specimens tested in this study, as will be discussed in the following sections.

Effect of Shear Span Length of Cantilevered CFFTs

Mechanically clamped end – Specimens C3 and the one tested by Fam and Mitchell (2010) were similar in test setup and fixed end arrangements. The main difference was the span lengths, which were 4.75D and 12.2D, respectively. It is noted from Figure 13 that the moment capacity of specimen C3 is only 7% lower than the other one, despite the significantly shorter span and hence the higher influence of shear. Given the variability of concrete fill strengths and the well established possibilities of variation of rupture strains of the tube, this 7% reduction is not significant enough to be attributed to the influence of higher shear forces. As such, it may be concluded that shear does not lead to reduction in flexural strength in fixed-end cantilevered CFFT members. This confirms the findings established earlier for CFFT simply supported beams by Ahmad et al. (2008).

Concrete footing for fixed end – Specimens C1 and C2 both had the same fixed-end arrangements and detailing, using a concrete footing. They had shear spans of 4.75D and 7.25D, respectively. While Specimen C1 with the shorter span achieved very close, but not quite, its potential flexural strength and failed at a moment of 49.2 kN.m (435 kip.in), Specimen C2, with the longer span, failed at a significantly lower moment of 30.2 kN.m (267 kip.in). It is important to note that both specimens failed by tensile rupture of the tube. It is also worth noting that the slip in Specimen C2 at failure was 11 mm (0.43 in), which is significantly larger than that in C1 at the same load level, 1.3 mm (0.05 in), as shown in Figure 12. The slip in Specimen C1 at failure was only 3 mm (0.12 in).

This behaviour is very significant; it clearly points out that achieving tension failure (rupture) of the tube does not guarantee achieving the full potential flexural moment capacity of the CFFT member. The reduction in moment capacity is clearly attributed to the influence of slip of the concrete core, at the critical maximum moment cross-section. The concrete core inside the tube, within the segment embedded in the footing was well anchored to the footing through the steel dowel bars. As such, the observed CFFT slip from the footing (Figure 11(b)) was in fact a slip of the GFRP tube, relative to both the external and internal concrete (i.e. the footing and the concrete core segment within the footing, respectively). This behaviour is illustrated in Figure 14(a). The result is widening of the internal flexural crack in the concrete core inside the tube at the footing face, due to that slip. This leads to significant reduction in the size of the intact concrete core compression zone, or even a complete separation in the entire concrete core at large slip, meaning a complete loss of the concrete compression zone.

The cross-section at this point could be somewhat similar to that of a hollow GFRP tube. This is supported by the observed very low moment capacity of specimen C2, which is in fact very close to that of the hollow tube tested by Fam and Mitchell (2010). This problem could be avoided either by embedding the CFRT an additional length inside the footing to reduce slip, or extending the steel dowels further into the CFRT.

It is important to note that a similar behaviour also occurs in short simply supported CFRT beams, where the unrestrained slip at the ends (Figure 11(a)) leads to a reduction of the concrete core compression zone size, as shown in Figure 14(b), and hence a reduction in moment capacity. However, because of the concrete arching action occurring in short and deep beams, the strength enhancement due to the arching action compensates for the weakening effect arising from the reduction of the compression zone size. The apparent result is no loss of the moment capacity or even a little gain as was observed in specimen B2 (based on low shear span and arching action), and also reported earlier by Ahmad et al. (2008).

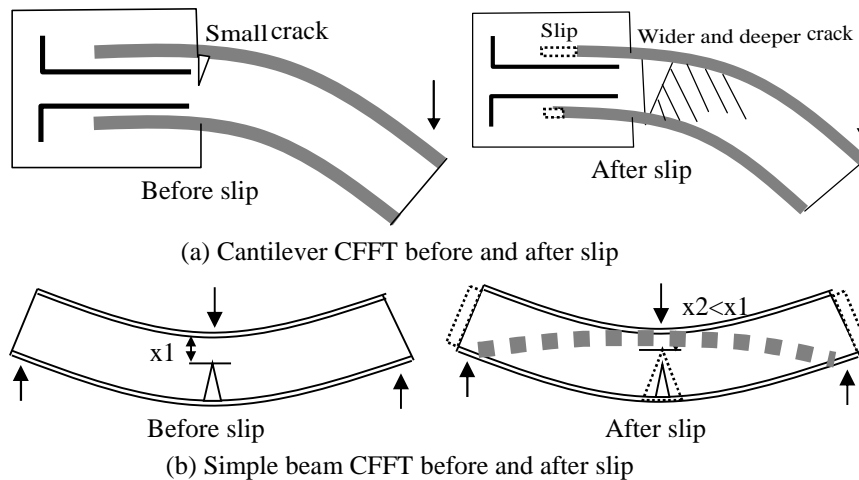


Figure 14 – Influence of concrete core slip on compression zone size

Effect of Fixed End Arrangement

Specimens C1 and C3 both had the same shear span of $4.75D$ but C1 had a moment connection through a concrete footing detailing, while C3 was mechanically clamped. In this case both specimens achieved a comparable moment capacity, with specimen C1 only 3.5% lower than C3, as shown in Figure 12. This suggests that the moment connection succeeded for this particular shear span length. However, clearly the premature failure of specimen C2 with the same moment connection but longer shear span suggests that the connection is vulnerable to significant slippage and cracking as the span gets longer.

CONCLUSIONS

In this study cantilevered CFFT members with different fixed end arrangements and different shear spans were tested. Additional CFFT control specimens were also tested as simply supported beams. The moment connections studied were a mechanically clamped fixed end and a CFFT embedment into a concrete footing with steel dowels extending from the footing into the concrete core of the CFFT, within the embedment length. The objectives of the study were to examine the effects of shear span length and moment connection detailing on flexural strength of CFFT cantilevered members. The following conclusions are drawn:

1. In short CFFT cantilevered members, the high level of shear does not cause shear failure or reduction in the ultimate moment capacity. A similar observation was reported in literature for simply supported CFFT beams.
2. Rupture of the GFRP tube in tension in the CFFT system is not necessarily an indication of achieving its full potential flexural strength. Slip between the concrete core and the tube in the vicinity of the moment connection could significantly reduce moment capacity, while the tube still failing in tension.
3. The effectiveness of the CFFT-footing moment connection studied reduces as the span of the CFFT member increases, due to the increased slip. The connection was successful in developing the full CFFT flexural strength for the span of 4.75D but not for the case of 7.25D, where only 40% of the flexural strength was achieved.

It is recommended that concrete footings of larger dimensions than those used in this study be used, to avoid cracking of the footing. It is also recommended that the CFFT embedment into the footing be increased or the steel dowels embedment into the concrete core of the CFFT member increase, to reduce the possibility of slip which could lead to reduction in moment capacity.

ACKNOWLEDGEMENTS

The authors wish to acknowledge the financial support provided by the Ontario Early Researcher Award program and the Queen's University Chancellor's Research Award. Special thanks go to Mark Nelson, Paul Thrasher, and Jaime Escobar from Queen's University.

REFERENCES

Ahmad, I., Zhu, Z., and Mirmiran, A., 2008, "Behavior of Short and Deep Beams Made of Concrete-Filled Fiber-Reinforced Polymer Tubes," *Journal of Composites for Construction*, ASCE, V. 12, No. 1, pp. 102-110.

Fam, A. Z. and Rizkalla, S. H., 2002, "Flexural Behaviour of Concrete-Filled Fiber-Reinforced Polymer Circular Tubes", *Journal of Composites for Construction*, ASCE, V. 6, No. 2, pp. 123-132.

Fam, A., Pando, M., Filz, G., and Rizkalla, S., 2003(b), "Precast Composite Piles for the Route 40 Bridge in Virginia Using Concrete-Filled FRP Tubes," *Precast Concrete Institute Journal*, V. 48, No. 3, pp. 32-45.

Fam, A., Flisak, B., and Rizkalla, S., 2003(a), "Experimental and Analytical Investigations of Concrete-Filled Fiber-Reinforced Polymer Tubes Subjected to Combined Bending and Axial Loads", *ACI Structural Journal*, V. 100, No. 4, pp. 499-509.

Fardis, M. N., and Khalili, H., 1981, "Concrete Encased in Fibreglass-Reinforced Plastic," *ACI Journal*, V. 78, No. 6, pp. 440-446.

Helmi, K., Fam, A., and Mufti, A., 2005, "Field installation, splicing, and flexural testing of hybrid FRP/concrete piles," *ACI Special Publication*, SP-230-62, pp. 1103-1120.

Mandal, S. K., 2004, "Prestressed Concrete-Filled Fiber Reinforced Polymer Tubes," M.Sc. Thesis, Queen's University, Kingston, Canada.

Mirmiran, A., and Shahawy, M., 1997, "Behavior of Concrete Columns Confined by Fiber Composites," *Journal of Structural Engineering*, ASCE, V. 123, No. 5, pp. 583-590.

Mitchell, J., and Fam, A., 2010, "Tests and Analysis of Cantilevered GFRP Tubular Poles with Partial Concrete Filling", *Journal of Composites for Construction*, ASCE, V. 14, No. 1, pp. 115-124.

Nelson, M., Lai, Y. C., and Fam, A., 2008, "Moment Connection of Concrete-Filled Fiber Reinforced Polymer Tubes by Direct Embedment into Footings," *Advances in Structural Engineering*, V. 11, No. 5, pp. 537-547.

Zhu, Z., Mirmiran, A., and Shahawy, M., 2004, "Stay-in-Place FRP Forms for Precast Modular Bridge Pier System." *Journal of Composites for Construction*, ASCE, V. 8, No. 6, pp. 560-568.

Zhu, Z., Ahmad, I., and Mirmiran, A., 2006, "Seismic Performance of Concrete-Filled FRP Tube Columns for Bridge Substructure," *Journal of Bridge Engineering*, ASCE, V. 11, No. 3, pp. 359-370.